

Measurement of mass attenuation coefficients, effective atomic numbers, and electron densities for different parts of medicinal aromatic plants in low-energy region

M. I. Sayyed¹ · F. Akman² · I. H. Geçibesler³ · H. O. Tekin⁴

Received: 17 March 2018 / Revised: 14 April 2018 / Accepted: 7 May 2018 / Published online: 30 August 2018
© Shanghai Institute of Applied Physics, Chinese Academy of Sciences, Chinese Nuclear Society, Science Press China and Springer Nature Singapore Pte Ltd. 2018

Abstract The mass attenuation coefficients (μ/ρ) for different parts (root, flower, stem, and leaf) of three medicinal aromatic plants (*Teucrium chamaedrys* L. subsp. *sinuatum*, *Rheum ribes*, and *Chrysophthalmum montanum*) were measured using an ²⁴¹Am photon source in a stable geometry and calculated using the Monte Carlo N-Particle Transport Code System-extended (MCNPX) code and the WinXCOM program. The experimental and theoretical MCNPX and WinXCOM values exhibited good agreement. The measured mass attenuation coefficient values were then used to compute the effective atomic number (Z_{eff}) and electron density (N_E) of the samples. The results reveal that S1-S (stem of *Teucrium chamaedrys* L. subsp. *sinuatum*) has the highest values of μ/ρ and Z_{eff} .

Keywords Medicinal · Aromatic plant · MCNPX code · Mass attenuation coefficient · Photon · WinXCOM

1 Introduction

Ionizing radiation is energy emitted from radioactive atoms in the form of particles (such as alpha, beta, and neutron) or electromagnetic waves (such as X-rays and gamma rays). Gamma rays and X-rays are chargeless and massless photons; thus, they are the most penetrating forms of ionizing radiation. Humans are exposed to ionizing radiation through different processes, such as diagnostic treatment of various cancers, nuclear power generation, and medical radiation exposure from X-rays. It is well known that exposure to ionizing radiation leads to the ionization of several biologically important macromolecules, including membranes, proteins, lipids, and nucleic acids [1, 2]. Ionizing radiation passing through living tissues results in the generation of reactive O species, which interact with DNA, causing cell damage, dysfunction, or death [3]. In recent decades, various studies have been performed to protect humans from the hurtful effects of ionizing radiation and to develop a novel and active radioprotector [4]. In this regard, numerous compounds have been investigated for their capability as a radioprotective material, such as vitamins, amino acids, plants, glasses, and herbs [4–9]. Radioprotective materials should be highly effective, cheap, orally administered, and without toxicity implications. Natural products such as plants have all of these properties. It is well known that medicinal plants are utilized in different traditional systems of medicine because they are considered non-toxic and are exceedingly accepted by people. The use of medicinal plants as radioprotective materials requires scientific evaluation and assessment. The precise values of photon interaction parameters, such as the mass attenuation coefficient and effective atomic number, are needed to clarify

✉ F. Akman
fakman@bingol.edu.tr

¹ Department of Physics, University of Tabuk, Tabuk 009662, Saudi Arabia

² Department of Electronic Communication Technology, Vocational School of Technical Sciences, Bingöl University, 12000 Bingöl, Turkey

³ Department of Occupational Health and Safety, Faculty of Health Science, Laboratory of Natural Product Research, Bingöl University, 12000 Bingöl, Turkey

⁴ Department of Radiotherapy, Üsküdar University, 34662 İstanbul, Turkey

the interaction of photons with medicinal plants. The mass attenuation coefficient (μ/ρ) for a medicinal plant indicates how easily it can be penetrated by a photon. This coefficient is considered to be one of the most important parameters characterizing the interaction between ionizing radiation and a specific medium and can be used to calculate other parameters, such as the effective atomic number and electron density [10, 11]. There are different methods for calculating the mass attenuation coefficients for a specific photon energy and material, including a theoretical approach employing the WinXCOM program [12], an experimental method using transmission geometry [13–15], and simulation codes such as Monte Carlo N-Particle Transport Code System-extended (MCNPX), Geant4, and FLUKA [10, 16, 17].

In the present study, we used the transmission geometry to measure the mass attenuation coefficients of different parts (root, flower, stem, and leaf) of three medicinal aromatic plants (*Teucrium chamaedrys* L. subsp. *sinuatum*, *Rheum ribes*, and *Chrysophthalmum montanum*). Additionally, we used the MCNPX code and the WinXCOM program to validate the obtained values. Using the obtained mass attenuation coefficients, we calculated related parameters, such as the effective atomic number and electron density.

2 Materials and methods

2.1 Sample preparation

Details regarding the localities of the plant samples used in the study are presented in Table 1. The samples were collected from natural habitats and transferred to the laboratory. The plant samples were divided into target organs while in the wet state. The target plant organs were allowed to be dried on unprinted papers in the laboratory. A laboratory-type mill was used to pulverize the dried plant samples. The powdered plant specimens were passed through a laboratory sieve and brought to a 20-mesh particle size. The milled plant samples were pelleted using a laboratory-type hydraulic pellet press.

The total organic content in the samples was analyzed using a spectrometer (FLASH 2000 Series CHNS/Organic Elemental Analyzer, Thermo Scientific). The total C, H, and N contents in each plant sample were determined according to the European standard EN15104:2011 [18], which suggests the following formula for the amount of O in the samples:

$$O (\%) = 100 - [C\% + H\% + N\%]_{(\text{LightestMoistBasis})} \quad (1)$$

The chemical compositions, densities, and codes of the present medicinal aromatic plants are listed in Table 2.

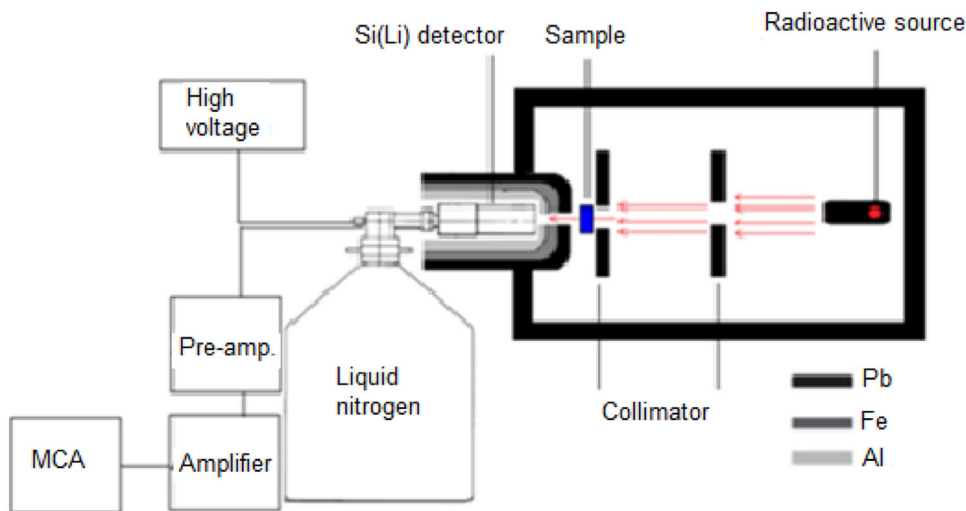
Table 1 Herbarium numbers, gathering times, localities, and coordinates of plant samples

Plant samples	Localities	Coordinates	Herbarium numbers	Gathering times
<i>Rheum ribes</i>	Bingöl-Yelesen village rocky slopes 1750 m	N: 38°52'09.2" E: 40°19'26.5"	KOCAK-4232	20.06.2017
<i>Chrysophthalmum montanum</i>	Diyarbakır-Kulp district vicinity, 1425 m	N: 38°30'23.3" E: 41°05'44.6"	KOCAK-4231	16.06.2016
<i>Teucrium chamaedrys</i> L. subsp. <i>sinuatum</i>	Bingöl-Sancak district and surrounding slopes 1550 m	N:39°10'31.2' E:40°22'16.8'	BIN-782	08.07.2016

Table 2 Chemical compositions of medicinal aromatic plants

Sample	Used part	Sample code	Density (g/cm ³)	H (%)	C (%)	N (%)	O (%)
<i>Teucrium chamaedrys</i> L. subsp. <i>sinuatum</i>	Root	S1-R	1.051	4.963	92.989	0.866	1.182
<i>Teucrium chamaedrys</i> L. subsp. <i>sinuatum</i>	Flower	S1-F	1.152	4.560	35.080	1.821	58.539
<i>Teucrium chamaedrys</i> L. subsp. <i>sinuatum</i>	Stem	S1-S	1.001	2.875	22.235	0.965	73.925
<i>Rheum ribes</i>	Stem	S2-S	1.273	6.702	40.663	0.871	51.764
<i>Rheum ribes</i>	Root	S2-R	1.135	4.368	65.964	0.736	28.932
<i>Rheum ribes</i>	Leaf	S2-L	1.001	11.448	47.435	2.425	38.691
<i>Chrysophthalmum montanum</i>	Stem	S3-S	1.367	5.308	51.544	0.674	42.474
<i>Chrysophthalmum montanum</i>	Leaf	S3-L	1.093	5.383	56.705	1.525	36.387
<i>Chrysophthalmum montanum</i>	Flower	S3-F	1.042	5.317	52.690	1.519	40.475

Fig. 1 Narrow-beam transmission geometry (Color online)



3 Experimental work

The spectrometer system comprised a Si(Li) semiconductor detector (SLP-04160P-OPT-0.3) having an energy resolution of 2.7% at 5.9 keV, a 12.5-mm² active area, and a 5-mm sensitive depth. A4 K multichannel analyzer was used to measure the mass attenuation coefficients of the medicinal aromatic plants. An ²⁴¹Am photon source having activity of 370 kBq was used to irradiate the plant samples. This source provided the following useful photon energies: 13.92, 17.75, 20.78, 26.34, and 59.54 keV.

The radioactive source enclosed in a lead cylinder with a 3-mm orifice was collimated to produce a narrow beam. The experimental narrow-beam geometry setup is shown in Fig. 1. The distance between the source and detector was 15 cm. The detector was housed in a lead shield to minimize the detection of background radiation from the surroundings. Each plant sample was placed between the source and detector. Then, the photon intensities I_0

(incident) and I (after attenuation) were measured by recording the corresponding counts for a fixed preset time. For each sample, gamma-ray intensities without (I_0) and after attenuation (I) were used to calculate the mass attenuation coefficients using the Lambert–Beer law [17]. More extensive information regarding the experimental process is presented in our previous works [19–21]. A typical spectrum of 13.92 keV with and without

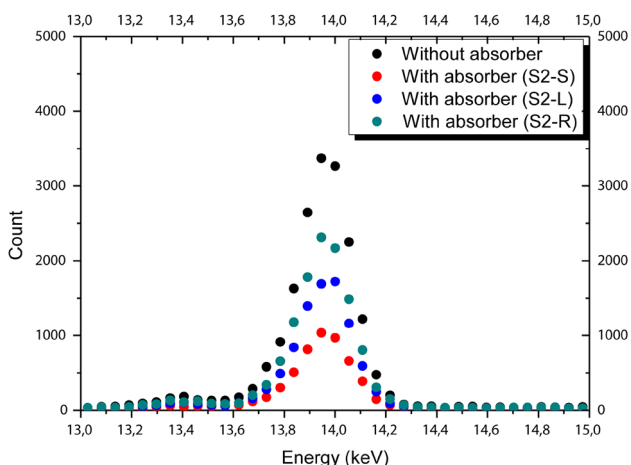


Fig. 2 A typical spectrum of 13.92 keV with and without attenuation by S2-S, S2-L and S2-R samples (Color online)

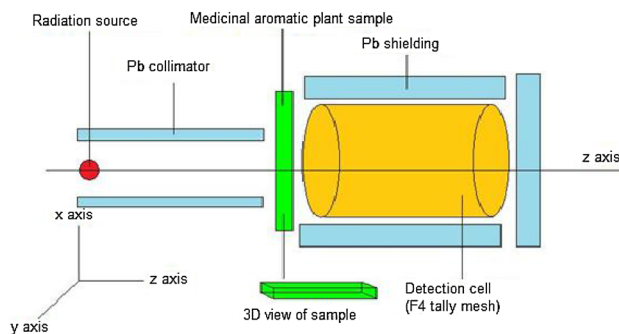


Fig. 3 Total simulation geometry of the present investigated samples (Color online)

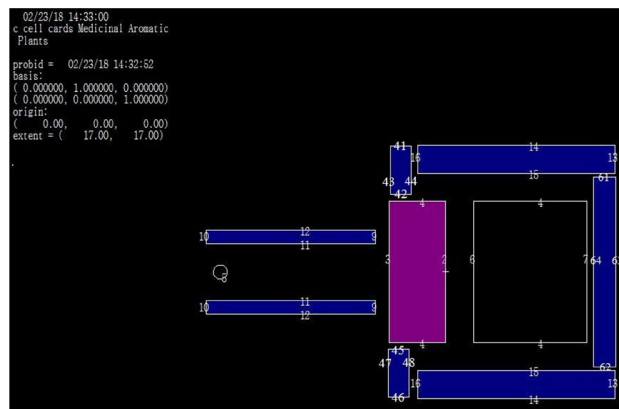


Fig. 4 Screenshot of MCNPX simulation setup (Color online)

attenuation by the S2-S, S2-L, and S2-R samples is shown in Fig. 2.

4 MCNPX code

The Monte Carlo method is one of the best ways to resolve physical problems, medical difficulties, and unknown parameters when the experimental or clinical

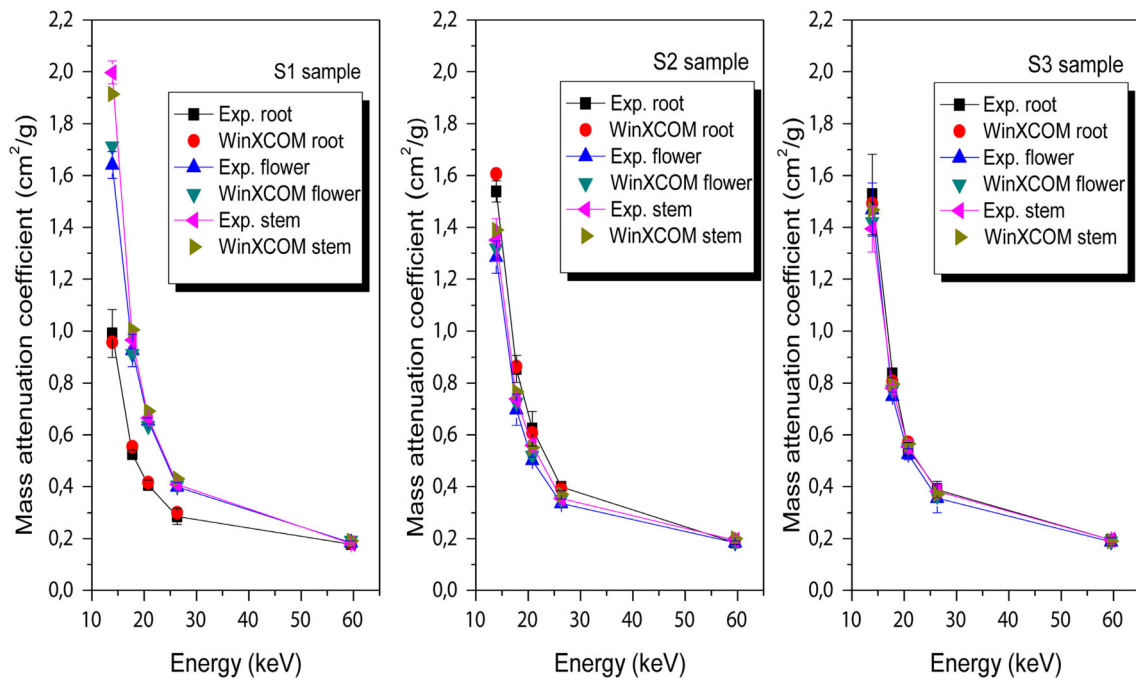


Fig. 5 Comparison of mass attenuation coefficients calculated by WinXCOM with respect to experiment for the present medicinal aromatic plants (Color online)

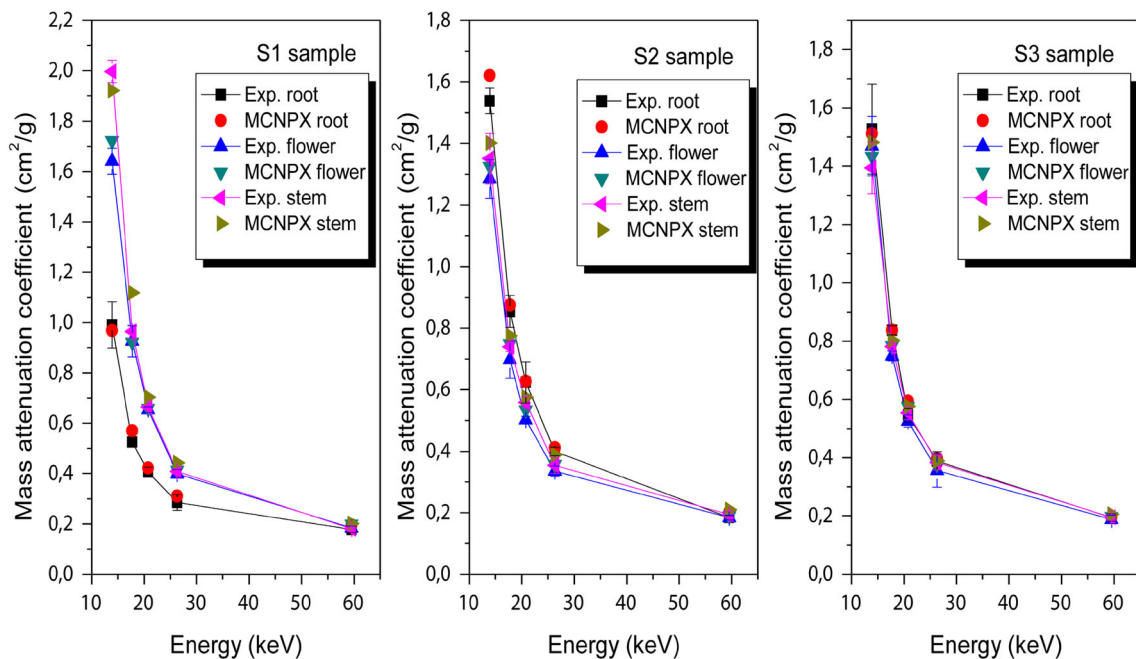


Fig. 6 Comparison of mass attenuation coefficients calculated by MCNPX code with respect to experiment for the present medicinal aromatic plants (Color online)

conditions are limited or difficult to attain. MCNPX version 2.6.0 (Los Alamos National Lab, USA) was utilized for the calculations of the mass attenuation coefficients of different parts of three medicinal aromatic plants. The MCNPX code is a general-purpose Monte Carlo radiation transport code for simulating the interaction of radiation with matter in a wide energy range [22]. MCNPX can ensure fully three-dimensional simulation and utilizes extended nuclear cross-section libraries and physics models for particle types. The validation of the MCNPX Monte Carlo code for the investigation of radiation mass attenuation coefficients and other shielding parameters for different types of materials—such as glasses, concrete, and living biological tissues—has been reported [23–33]. The computational modeling of radiation interaction problems, including the radiation attenuation and shielding properties, depends on the material definitions. The input structure of the MCNPX code has three major parts defining the significant details of the simulation. A completed MCNPX input file describes the problem geometry and defines the materials with their chemical compositions, as well as the structure of the radiation source, including details such as the source geometry and radiation distribution. The simulation geometry is constructed by defining cells. Each cell in the simulation is bounded by one or more geometric surfaces. In the present investigation, the square prism geometry was employed for modeling the parts of medicinal aromatic plants. The edge lengths of this square prism geometry were defined as 5 cm, while the axial z-length was set differently for each simulation because it represents the thickness of the parts of the medicinal aromatic plants. The mass attenuation coefficients of each part of the medicinal aromatic plant sample were measured in a narrow-beam transmission geometry using a point isotropic source with a collimated and monoenergetic beam. The radiation energy value of the point isotropic source was defined in the photon energy range of 13.92–59.54 keV for each calculation. The geometric center of the detection area on the central axis was considered as the location of the point isotropic source that emits gamma rays perpendicular to the front face of the medicinal aromatic plant sample in the direction of the z-axis. Another important definition is the material definition, considering the atomic number, mass number, elemental mass fraction, and density of compounds or mixtures. The elemental mass fractions and densities of each medicinal aromatic plant sample are presented in Table 2. In the present MCNPX simulation, to obtain the absorbed dose amount in the detection field, the average flux tally (F4) was utilized. This type of tally mash gives the sum of the average flux in the cell. The initial quantity of gamma rays is set as 10^8 particles. The mass attenuation coefficient calculations were performed using Intel® Core™ i7 CPU 2.80 GHz

Table 3 Experimental and theoretical values of mass attenuation coefficient for medicinal aromatic plants

Code	13.92 keV		17.75 keV		20.78 keV		26.34 keV		59.54 keV						
	Exp	WinX MCNPX	Exp	WinX MCNPX	Exp	WinX MCNPX	Exp	WinX MCNPX	Exp	WinX MCNPX					
S1-R	0.990 ± 0.092	0.957	0.969	0.526 ± 0.015	0.555	0.570	0.407 ± 0.020	0.416	0.423	0.285 ± 0.031	0.300	0.310	0.178 ± 0.013	0.184	0.195
S1-F	1.641 ± 0.052	1.713	1.722	0.926 ± 0.062	0.912	0.922	0.654 ± 0.012	0.636	0.659	0.400 ± 0.016	0.405	0.413	0.184 ± 0.008	0.192	0.200
S1-S	1.997 ± 0.044	1.914	1.921	0.965 ± 0.025	1.005	1.118	0.665 ± 0.007	0.692	0.703	0.409 ± 0.010	0.431	0.443	0.181 ± 0.005	0.192	0.201
S2-S	1.538 ± 0.041	1.606	1.621	0.854 ± 0.052	0.863	0.875	0.624 ± 0.067	0.607	0.627	0.400 ± 0.014	0.393	0.627	0.184 ± 0.007	0.194	0.201
S2-R	1.285 ± 0.063	1.319	1.326	0.698 ± 0.061	0.726	0.749	0.502 ± 0.011	0.521	0.534	0.335 ± 0.017	0.350	0.534	0.184 ± 0.008	0.187	0.190
S2-L	1.351 ± 0.082	1.390	1.401	0.739 ± 0.014	0.766	0.776	0.559 ± 0.017	0.551	0.576	0.354 ± 0.026	0.371	0.576	0.193 ± 0.012	0.200	0.210
S3-S	1.528 ± 0.155	1.491	1.511	0.837 ± 0.016	0.808	0.837	0.546 ± 0.024	0.572	0.595	0.389 ± 0.032	0.375	0.397	0.194 ± 0.013	0.191	0.195
S3-L	1.469 ± 0.102	1.420	1.433	0.749 ± 0.017	0.774	0.785	0.526 ± 0.021	0.551	0.575	0.356 ± 0.057	0.365	0.378	0.188 ± 0.014	0.190	0.199
S3-F	1.394 ± 0.088	1.468	1.481	0.781 ± 0.012	0.797	0.803	0.544 ± 0.023	0.565	0.577	0.383 ± 0.025	0.372	0.389	0.195 ± 0.011	0.190	0.206

computer hardware. The error rate in the output file was observed to be $< 0.1\%$. Analysis of a recent investigation was performed using the D00205ALLCP03 MCNPXDATA package, which comprises DLC-200/MCNPDATA cross-section libraries. This library typically includes ENDF/B-VI data in the range of 20–150 MeV. Figure 3 shows the total simulation geometry for the present investigation. A screenshot showing the design of the MCNPX simulation setup is displayed in Fig. 4.

5 Results and discussion

Different photon attenuation coefficients—such as the mass attenuation coefficients (μ/ρ), effective atomic number (Z_{eff}), and electron density (N_e)—of different parts (root, flower, stem, and leaf) of three medicinal aromatic plants (*Teucrium chamaedrys* L. subsp. *sinuatum*, *Rheum ribes*, and *Chrysophthalmum montanum*) were investigated. The μ/ρ values of the present samples were obtained in three ways: (a) experimentally, using a transmission arrangement; (b) theoretically, using the WinXCOM program; and (c) using a Monte Carlo simulation (MCNPX code). The experimental and WinXCOM results for the μ/ρ of the present samples at 13.92, 17.75, 20.78, 26.34, and 59.54 keV are illustrated in Fig. 5, while the experimental and MCNPX results for the μ/ρ of all the samples are shown in Fig. 6. The experimental, WinXCOM, and MCNPX results for the μ/ρ are summarized in Table 3.

The tendency of μ/ρ is almost the same for all samples owing to the similarity of the elemental compositions among the samples (all the samples contain H, C, N, and O in different proportions).

Figures 5 and 6 clearly show that the experimentally measured μ/ρ values of the medicinal aromatic plants agree well with the WinXCOM and MCNPX results. The present experimental WinXCOM and MCNPX results are similar to the observations of Singh et al. [25], who studied the μ/ρ of polymers in the energy range of 59.5–1332.5 MeV using Monte Carlo simulation (MCNP-4C) and reported good agreement among their MCNP-4C, XCOM, and experimental results. The μ/ρ values for all samples decrease with the increase of the photon energy. This means that with the increase of the energy of the incident photons, we obtain smaller attenuation; thus, more photons can penetrate the present samples.

The differences among the μ/ρ values due to the medicinal aromatic plant compositions are obvious, particularly in the low-energy region. As shown in Table 3, S1-S (stem of *Teucrium chamaedrys* L. subsp. *sinuatum*) has higher values of μ/ρ than the other samples because of the larger amount of O in this sample (73.925%). Additionally, Table 3 shows that the S1-R sample has the lowest μ/ρ values, as this sample contains mainly C (92.989%), while the percent of O in this sample is low (1.182%). It is important to investigate the experimental uncertainty in the measurement of μ/ρ . The following equation was used for this:

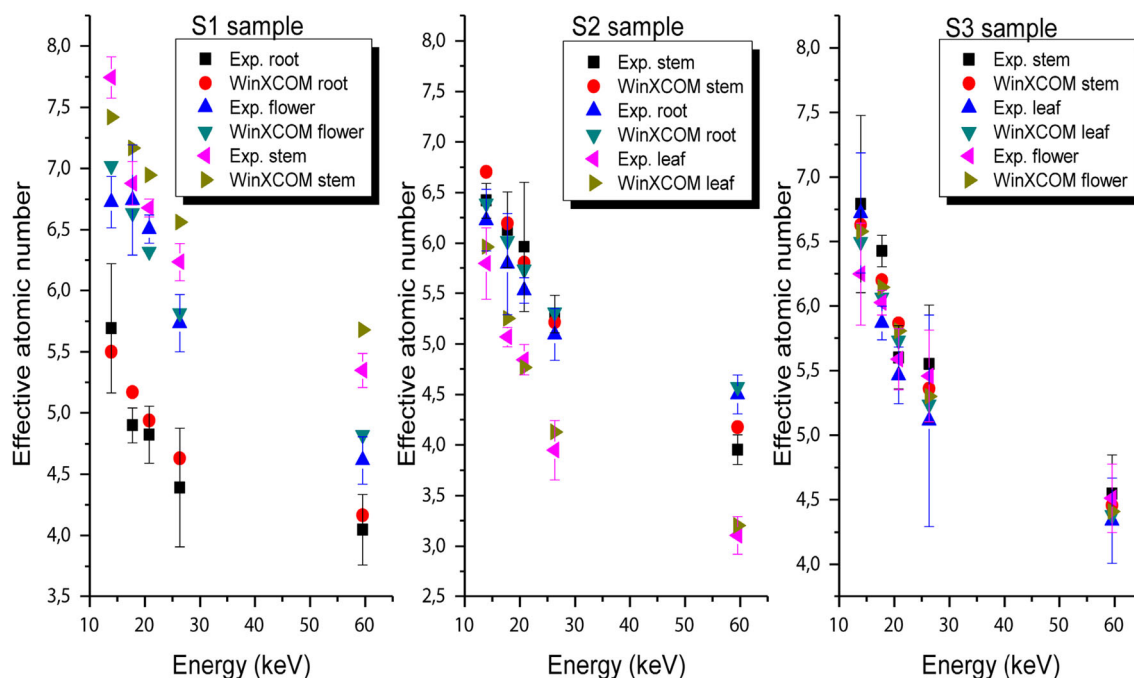


Fig. 7 Experimentally measured effective atomic numbers for the present medicinal aromatic plants in comparison with those obtained by WinXCOM (Color online)

Table 4 Experimental and theoretical values of effective atomic number for medicinal aromatic plants

Code	13.92 keV		17.75 keV		20.78 keV		26.34 keV		59.54 keV	
	Exp	Theo								
S1-R	5.692 ± 0.527	5.500	4.900 ± 0.142	5.169	4.824 ± 0.232	4.938	4.392 ± 0.484	4.630	4.047 ± 0.288	4.164
S1-F	6.725 ± 0.211	7.022	6.740 ± 0.452	6.637	6.506 ± 0.115	6.321	5.734 ± 0.234	5.816	4.613 ± 0.194	4.821
S1-S	7.744 ± 0.169	7.420	6.880 ± 0.178	7.167	6.678 ± 0.073	6.945	6.235 ± 0.154	6.561	5.348 ± 0.138	5.678
S2-S	6.419 ± 0.172	6.703	6.130 ± 0.376	6.195	5.961 ± 0.640	5.801	5.294 ± 0.186	5.212	3.954 ± 0.146	4.176
S2-R	6.226 ± 0.303	6.391	5.790 ± 0.502	6.020	5.528 ± 0.125	5.735	5.092 ± 0.256	5.311	4.499 ± 0.192	4.575
S2-L	5.795 ± 0.354	5.962	5.067 ± 0.096	5.252	4.843 ± 0.150	4.768	3.949 ± 0.294	4.130	3.107 ± 0.185	3.205
S3-S	6.790 ± 0.688	6.629	6.427 ± 0.122	6.199	5.601 ± 0.244	5.864	5.552 ± 0.454	5.358	4.547 ± 0.301	4.456
S3-L	6.720 ± 0.466	6.499	5.868 ± 0.130	6.066	5.463 ± 0.219	5.733	5.112 ± 0.818	5.239	4.338 ± 0.329	4.382
S3-F	6.247 ± 0.396	6.580	6.025 ± 0.096	6.144	5.588 ± 0.236	5.806	5.458 ± 0.355	5.300	4.512 ± 0.265	4.409

$$\Delta\left(\frac{\mu}{\rho}\right) = \frac{1}{\rho x} \sqrt{\left(\frac{\Delta I_0}{I_0}\right)^2 + \left(\frac{\Delta I}{I}\right)^2 + \left(\ln \frac{I_0}{I}\right)^2 \cdot \left(\frac{\Delta \rho x}{\rho x}\right)^2}, \quad (2)$$

where x and ρ represent the thickness and density of the sample, respectively, and ΔI_0 and ΔI are the uncertainties of I_0 and I , respectively.

Equation (2) was used to calculate the experimental uncertainty in the measurement of μ/ρ , and the results are summarized in Table 3. Clearly, the uncertainties in the experimental μ/ρ measurements are within the range of

1.09% to 10.73% (except for S1-R and S3-F at 26.34 keV). The uncertainties in the measurements are mainly due to statistical uncertainties in the determination of the intensity without (I_0) and with (I) the absorber, as well as to the scattered photons reaching the detector.

By using the measured and calculated data for μ/ρ , the effective atomic numbers (Z_{eff}) were calculated as follows [34]:

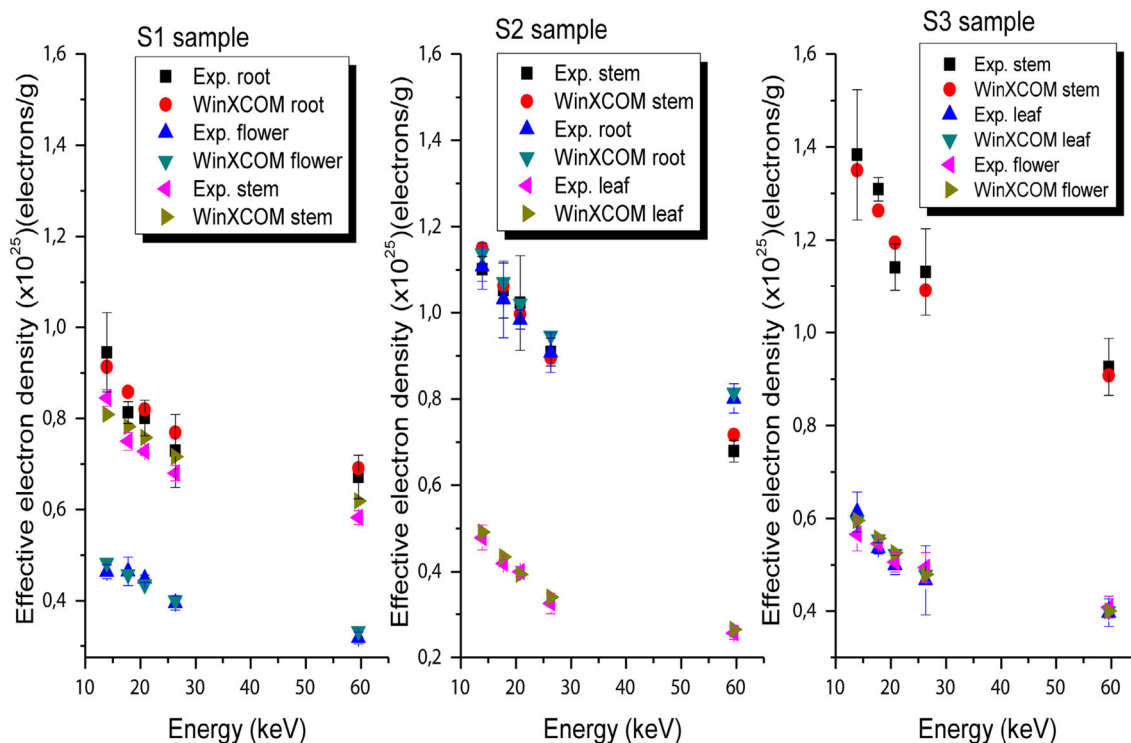


Fig. 8 Experimentally measured effective electron densities for the present medicinal aromatic plants in comparison with those obtained by WinXCOM (Color online)

Table 5 Experimental and theoretical values of effective electron density ($\times 10^{25}$) for medicinal aromatic plants

Code	13.92 keV		17.75 keV		20.78 keV		26.34 keV		59.54 keV	
	Exp	Theo								
S1-R	0.945 ± 0.087	0.913	0.813 ± 0.024	0.858	0.801 ± 0.039	0.820	0.729 ± 0.080	0.769	0.672 ± 0.048	0.691
S1-F	0.464 ± 0.015	0.484	0.465 ± 0.031	0.458	0.449 ± 0.008	0.436	0.395 ± 0.016	0.401	0.318 ± 0.013	0.333
S1-S	0.845 ± 0.018	0.809	0.750 ± 0.019	0.782	0.728 ± 0.008	0.758	0.680 ± 0.017	0.716	0.583 ± 0.015	0.619
S2-S	1.102 ± 0.029	1.150	1.052 ± 0.064	1.063	1.023 ± 0.110	0.996	0.909 ± 0.032	0.895	0.679 ± 0.025	0.717
S2-R	1.108 ± 0.054	1.138	1.031 ± 0.089	1.072	0.984 ± 0.022	1.021	0.907 ± 0.046	0.946	0.801 ± 0.034	0.815
S2-L	0.479 ± 0.029	0.492	0.419 ± 0.008	0.434	0.400 ± 0.012	0.394	0.326 ± 0.024	0.341	0.257 ± 0.015	0.265
S3-S	1.383 ± 0.140	1.350	1.309 ± 0.025	1.263	1.141 ± 0.050	1.194	1.131 ± 0.093	1.091	0.926 ± 0.061	0.908
S3-L	0.614 ± 0.043	0.594	0.536 ± 0.012	0.555	0.500 ± 0.020	0.524	0.467 ± 0.075	0.479	0.397 ± 0.030	0.401
S3-F	0.566 ± 0.036	0.596	0.546 ± 0.009	0.557	0.506 ± 0.021	0.526	0.495 ± 0.032	0.480	0.409 ± 0.024	0.400

$$Z_{\text{eff}} = \frac{\sum_i f_i A_i (\mu/\rho)_i}{\sum_j f_j \frac{A_j}{Z_j} (\mu/\rho)_j} \quad (3)$$

where f_i represents the fractional abundance of the element i relative to the number of atoms, and Z_i and A_i are the atomic number and atomic weight, respectively. The results for the Z_{eff} of the selected samples are plotted with respect to the photon energy in Fig. 7. In addition, the experimental Z_{eff} values are presented in Table 4, together with theoretical values. The Z_{eff} results indicate good agreement between the experiment and theory. As shown in Table 4, the values of Z_{eff} for all the medicinal aromatic plants change with respect to the photon energy. In the case of *Teucrium chamaedrys* L. subsp. *sinuatum*, Z_{eff} ranges from 5.692 to 4.047, 6.725 to 4.613, and 7.744 to 5.348 for the root, flower, and stem, respectively. In the case of *Rheum ribes*, Z_{eff} ranges from 6.419 to 3.954, 6.226 to 4.499, and 5.795 to 3.107 for the stem, root, and leaf, respectively. In the case of *Chrysophthalmum montanum*, Z_{eff} ranges from 6.790 to 4.547, 6.720 to 4.338, and 6.247 to 4.512 for the stem, leaf, and flower, respectively. Notably, the atomic numbers (Z) of the elements of the present medicinal aromatic plants change from 1 (H) to 8 (O), and a total of four elements (H, C, N, and O) are considered. The values of Z_{eff} for the present plants lie within the range of Z for the constituent elements ($1 < Z_{\text{eff}} < 8$). As indicated by the μ/ρ results, S1-S (stem of *Teucrium chamaedrys* L. subsp. *sinuatum*) has higher values of Z_{eff} .

Z_{eff} is related to another parameter called the effective electron density (N_E), which represents the number of electrons per unit mass of the interacting materials and can be calculated using the following relation [35]:

$$N_E = N_A \frac{n_{\text{tot}} Z_{\text{eff}}}{\sum_i n_i A_i} = N_A \frac{Z_{\text{eff}}}{\langle A \rangle} \quad (4)$$

where $\langle A \rangle$ is the mean atomic mass, and N_A is the Avogadro constant. The determined N_E for the present samples is plotted in Fig. 8 and listed in Table 5. As shown in Fig. 8, the experimental and theoretical (WinXCOM) values agree well. It is also clear from Fig. 8 that the N_E for all samples decreases with increasing energy owing to the dominance of the photoelectric effect in this energy region.

6 Conclusion

This work aimed to measure the mass attenuation coefficient (μ/ρ) for different parts (root, flower, stem, and leaf) of three medicinal aromatic plants using an ^{241}Am photon source in a stable geometry. The μ/ρ for all samples under investigation was also calculated using the MCNPX code and the WinXCOM program. The μ/ρ values obtained using the three aforementioned methods were similar. Furthermore, the effective atomic numbers (Z_{eff}) and the electron densities (N_E) for the medicinal aromatic plants were calculated. The calculations indicate that S1-S (stem of *Teucrium chamaedrys* L. subsp. *sinuatum*) has the highest values of μ/ρ and Z_{eff} . The numerical methods and simulation tools employed in this study can be very useful for similar future studies, particularly for cases where it is not possible to perform experimental studies. Monte Carlo simulations are a viable alternative method when experimental investigations are not possible. The recent Monte Carlo method can encourage the scientific community to undertake similar studies and to better evaluate the biological structures and their radiation interaction properties.

References

1. K.B. Kalpana, N. Devipriya, M. Srinivasan et al., Evaluating the radioprotective effect of hesperidin in the liver of Swiss albino mice. *Eur. J. Pharmacol.* **658**, 206–212 (2011). <https://doi.org/10.1016/j.ejphar.2011.02.031>
2. K.B. Kalpana, N. Devipriya, M. Srinivasan et al., Investigation of the radioprotective efficacy of hesperidin against gamma-radiation induced cellular damage in cultured human peripheral blood lymphocytes. *Mutat. Res.* **676**, 54–61 (2009). <https://doi.org/10.1016/j.mrgentox.2009.03.005>
3. W. Lee, W. Kang, N. Kim et al., Radioprotective effects of a polysaccharide purified from *Lactobacillus plantarum*-fermented *Ishigeokamurae* against oxidative stress caused by gamma ray-irradiation in zebrafish in vivo model. *J. Funct. Food* **28**, 83–89 (2017). <https://doi.org/10.1016/j.jff.2016.11.004>
4. S.J. Hosseinimehr, Trends in the development of radioprotective agents. *Drug Discov. Today* **12**, 794–805 (2007). <https://doi.org/10.1016/j.drudis.2007.07.017>
5. A. Pezeshk, The effects of ionizing radiation on DNA: the role of thiols as radioprotectors. *Life Sci.* **74**, 2423–2429 (2004). <https://doi.org/10.1016/j.lfs.2003.09.068>
6. R. Arora, D. Gupta, R. Chawla et al., Radioprotection by plant products: present status and future prospects. *Phytother. Res.* **19**, 1–22 (2005). <https://doi.org/10.1002/ptr.1605>
7. M. Kurudirek, Effective atomic numbers, water and tissue equivalence properties of human tissues, tissue equivalents and dosimetric materials for total electron interaction in the energy region 10 keV–1 GeV. *Appl. Radiat. Isot.* **94**, 1–7 (2014). <https://doi.org/10.1016/j.apradiso.2014.07.002>
8. M. Kurudirek, Effective atomic numbers of different types of materials for proton interaction in the energy region 1 keV–10 GeV. *Nucl. Instrum. Methods B* **336**, 130–134 (2014). <https://doi.org/10.1016/j.nimb.2014.07.008>
9. M. Kurudirek, T. Onaran, Calculation of effective atomic number and electron density of essential biomolecules for electron, proton, alpha particle and multi-energetic photon interactions. *Radiat. Phys. Chem.* **112**, 125–138 (2015). <https://doi.org/10.1016/j.radphyschem.2015.03.034>
10. G. Lakshminarayana, A. Kumar, M.G. Dong et al., Exploration of gamma radiation shielding features for titanate bismuth borotellurite glasses using relevant software program and Monte Carlo simulation code. *J. Non Cryst. Solids* **481**, 65–73 (2018). <https://doi.org/10.1016/j.jnoncrysol.2017.10.027>
11. A. Kumar, M.I. Sayyed, M. Dong et al., Effect of PbO on the shielding behavior of ZnO–P2O5 glass system using Monte Carlo simulation. *J. Non Cryst. Solids* **48**, 604–607 (2018). <https://doi.org/10.1016/j.jnoncrysol.2017.12.001>
12. L. Gerward, N. Guilbert, K.B. Jensen et al., WinXCom – a program for calculating X-ray attenuation coefficients. *Radiat. Phys. Chem.* **71**, 653–654 (2004). <https://doi.org/10.1016/j.radphyschem.2004.04.040>
13. J. Kaewkhao, J. Laopaiboon, W. Chewpraditkul, Determination of effective atomic numbers and effective electron densities for Cu/Zn alloy. *J. Quant. Spectrosc. Radiat.* **109**, 1260–1265 (2008). <https://doi.org/10.1016/j.jqsrt.2007.10.007>
14. S. Seven, I.H. Karahan, Ö.F. Bakkaloglu, The measurement of total mass attenuation coefficients of CoCuNi alloys. *J. Quant. Spectrosc. Radiat.* **83**, 237–242 (2004). [https://doi.org/10.1016/S0022-4073\(03\)00118-3](https://doi.org/10.1016/S0022-4073(03)00118-3)
15. M. Dong, X. Xue, A. Kumar et al., A novel method of utilization of hot dip galvanizing slag using the heat waste from itself for protection from radiation. *J. Hazard. Mater.* **344**, 602–614 (2018). <https://doi.org/10.1016/j.jhazmat.2017.10.066>
16. B.O. Elbashir, M.G. Dong, M.I. Sayyed et al., Comparison of Monte Carlo simulation of gamma ray attenuation coefficients of amino acids with XCOM program and experimental data. *Results Phys.* **9**, 6–11 (2018). <https://doi.org/10.1016/j.rinp.2018.01.075>
17. M.I. Sayyed, M.Y. AlZaatreh, M.G. Dong et al., A comprehensive study of the energy absorption and exposure buildup factors of different bricks for gamma-rays shielding. *Results Phys.* **7**, 2528–2533 (2017). <https://doi.org/10.1016/j.rinp.2017.07.028>
18. British Standards Institute – BSI (2011): Solid Biofuels Standards n°EN 14774-1:2009, EN 14775:2009, EN 15148:2009, EN 15104:2011, EN 15289:2011 [online]. <http://www.standards.ie> (Accessed 21 January 2011)
19. F. Akman, R. Durak, M.R. Kaçal et al., Study of absorption parameters around the K edge for selected compounds of Gd. *X Ray Spectrom.* **45**(2), 103–110 (2016). <https://doi.org/10.1002/xrs.2676>
20. F. Akman, R. Durak, M.F. Turhan et al., Studies on effective atomic numbers, electron densities from mass attenuation coefficients near the K edge in some samarium compounds. *Appl. Radiat. Isot.* **101**, 107–113 (2015). <https://doi.org/10.1016/j.apradiso.2015.04.001>
21. F. Akman, M.R. Kaçal, F. Akman et al., Determination of effective atomic numbers and electron densities from mass attenuation coefficients for some selected complexes containing lanthanides. *Can. J. Phys.* **95**(10), 1005–1011 (2017). <https://doi.org/10.1139/cjp-2016-0811>
22. RSICC computer code collection. MCNPX user's manual version 2.4.0. Monte Carlo n-particle transport code system for multiple and high energy applications, 2002
23. H.O. Tekin, MCNP-X Monte Carlo Code application for mass attenuation coefficients of concrete at different energies by modeling 3X3inch NaI(Tl) detector and comparison with XCOM and Monte Carlo Data. *Sci. Technol. Nucl. Install.* **2016**, (2016). <http://dx.doi.org/10.1155/2016/6547318>
24. I. Akkurt, H.O. Tekin, A. Mesbahi, Calculation of detection efficiency for the gamma detector using MCNPX. *Acta Phys. Pol. A* **128**, 332–334 (2015). <https://doi.org/10.12693/APhysPolA.128.B-332>
25. V.P. Singh, S.P. Shirmardi, M.E. Medhat et al., Determination of mass attenuation coefficient for some polymers using Monte Carlo simulation. *Vacuum* **119**, 284–288 (2015). <https://doi.org/10.1016/j.vacuum.2015.06.006>
26. A.M. El-Khayatt, A.M. Ali, V.P. Singh, Photon attenuation coefficients of heavy-metal oxide glasses by MCNP code, XCOM program and experimental data: a comparison study. *Nucl. Instrum. Methods A* **735**, 207–212 (2014). <https://doi.org/10.1016/j.nima.2013.09.027>
27. H.O. Tekin, V.P. Singh, T. Manici, Effects of micro-sized and nano-sized WO3 on mass attenuation coefficients of concrete by using MCNPX code. *Appl. Radiat. Isot.* **121**, 122–125 (2017). <https://doi.org/10.1016/j.apradiso.2016.12.040>
28. A. Mesbahi, H. Ghiasi, Shielding properties of the ordinary concrete loaded with micro- and nanoparticles against neutron and gamma radiations. *Appl. Radiat. Isot.* **136**, 27–31 (2018). <https://doi.org/10.1016/j.apradiso.2018.02.004>
29. H.O. Tekin, V.P. Singh, T. Manici et al., Validation of MCNPX with experimental results of mass attenuation coefficients for cement, gypsum and mixture. *J. Radiat. Prot. Res.* **42**, 154–157 (2017). <https://doi.org/10.14407/jrpr.2017.42.3.154>
30. M.G. Dong, R. El-Mallawany, M.I. Sayyed et al., Shielding properties of 80TeO2–5TiO2–(15-x)WO3–xA_nO_m glasses using WinXCom and MCNP5 code. *Radiat. Phys. Chem.* **141**, 172–178 (2017). <https://doi.org/10.1016/j.radphyschem.2017.12.012>
31. G. Lakshminarayana, S.O. Baki, K.M. Kaky et al., Investigation of structural, thermal properties and shielding parameters for multicomponent borate glasses for gamma and neutron radiation

- shielding applications. *J. Non. Cryst. Solids.* **471**, 222–237 (2017). <https://doi.org/10.1016/j.jnoncrysol.2017.06.001>
32. H.O. Tekin, M.I. Sayyed, E.E. Altunsoy et al., Shielding properties and effects of WO₃ and PbO on mass attenuation coefficients by using MCNPX code. *Dig. J. Nanomater. Biostruct.* **12**, 861–867 (2017)
 33. H.O. Tekin, M.I. Sayyed, T. Manici et al., Photon shielding characterizations of bismuth modified borate—silicate-tellurite glasses using MCNPX Monte Carlo code. *Mater. Chem. Phys.* **211**, 9–16 (2018). <https://doi.org/10.1016/j.matchemphys.2018.02.009>
 34. M.I. Sayyed, H. Elhouichet, Variation of energy absorption and exposure buildup factors with incident photon energy and penetration depth for boro-tellurite (B₂O₃-TeO₂) glasses. *Radiat. Phys. Chem.* **130**, 335–342 (2017). <https://doi.org/10.1016/j.radphyschem.2016.09.019>
 35. M. Kurudirek, Effective atomic numbers and electron densities of some human tissues and dosimetric materials for mean energies of various radiation sources relevant to radiotherapy and medical applications. *Radiat. Phys. Chem.* **102**, 139–146 (2014). <https://doi.org/10.1016/j.radphyschem.2014.04.033>